Induced Effects in a Pacemaker Equipped With a Wireless Power Transfer Charging System

T. Campi[1], S. Cruciani[1], V. De Santis[1], F. Palandrani[1], F. Maradei[2], and M. Feliziani[1]

[1]Department of Industrial and Information Engineering and Economics, University of L'Aquila, 67100 L'Aquila, Italy
[2]Department of Astronautics, Electrical and Energetic Engineering, Sapienza University of Rome, 00185 Rome, Italy

This paper deals with the intrasystem electromagnetic interference (EMI) in a pacemaker equipped with a wireless power transfer (WPT) charging system. The WPT application to pacemakers is very new, and no results are yet published on possible EMI effects produced by the WPT coil currents in the pacemaker pacing leads. To this aim, an efficient and original co-simulation circuit/field method is proposed to predict the induced voltages on a pacing lead. In the numerical calculation, the pacemaker with WPT secondary coil and a pacing lead is implanted in a sophisticated human body model. The numerical results are validated by measurements showing a good agreement. The proposed approach would be a useful tool for pacemaker EMI compliance tests and safety assessment evaluations.

Index Terms— **Coupling, electromagnetic compatibility, leads, pacemakers, transmission line (TL), wireless power transfer.**

I. Introduction

THE usage of wireless power transfer (WPT) to recharge the battery of pacemakers or active implanted medical devices has been recently envisaged [1]–[4]. While system design and electromagnetic field (EMF) safety aspects have been addressed in [1] and [2], the electromagnetic interference (EMI) produced by the WPT system on the pacemaker itself is hereby considered for the first time. The WPT coil currents produce a time-varying magnetic field that can induce current and voltage on the pacing leads, which in turn can generate interference in the circuitry of the pacemaker itself and, above all, can inject current in the heart [5], [6]. The main coupling mechanism between the pacemaker and the magnetic field generated by the WPT system is due to the loop formed by the lead system through the human tissues (see Fig. 1). This loop area depends on the electro-geometrical configuration of the pacing leads.

Due to the complexity of the configuration composed by the human body, pacing leads, WPT coils, and pacemaker housing, a full numerical investigation is not practicable. To overcome this difficulty, a circuit-field co-simulation tool is proposed to evaluate the voltage induced at the input port of the pacemaker. In the proposed approach, the configuration of the pacemaker with a unipolar lead is modeled by an equivalent circuit obtained applying the transmission line (TL) theory, while the software tool COMSOL is used to derive the circuit parameters. This technique allows a fast calculation of the induced voltage for several lead types and electro-geometrical configurations.

II. System Configuration

When a pacemaker is equipped with a WPT charging system, the primary coil is located on the body surface, while the secondary coil is inside the body, i.e., in the pacemaker [1], [2]. The WPT coil currents produce a time-varying magnetic field needed to inductively transfer power, but this field can also induce currents and voltages on the pacing leads with the risk to generate EMI in the pacemaker circuitry and problems to the heart [5]–[9].

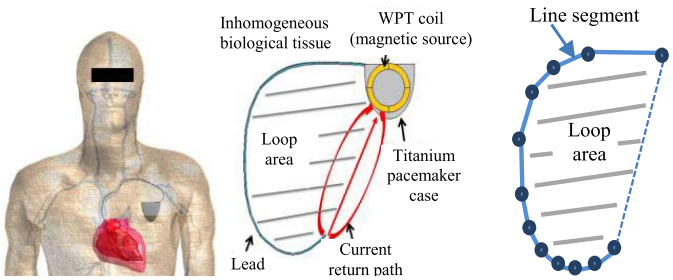

Fig. 1. (a) Pacemaker with a unipolar lead implanted on a realistic anatomical model. (b) Sketch of current return path and loop area. (c) Lead discretization.

When considering a pacemaker with a unipolar lead, the pacemaker has the cathode electrode that lies within the heart while the anode is the metallic housing of the pacemaker [see Fig. 1(a)]. The current return path inside the human body is not clearly defined, as shown in Fig. 1(b). In the proposed method, the unipolar lead is assumed to be a field-excited nonuniform TL. Thus, the lead is discretized in a number of series-connected TL segments as shown in Fig. 1(c), whose excitation depends mainly on the loop area delimited by the lead and the current return path.

III. Mathematical Model

A. Equivalent Circuits

After the unipolar lead discretization, the equivalent circuit of the field excited TL can be modeled by a series cascade of lumped parameter active two-port networks. The lumped equivalent circuit of the ith lead section in frequency domain is shown in Fig. 2(a), where $Z_{ii} = R_i + j\omega L_{ii}$ is the series impedance, $Y_{ii} = G_i + j\omega C_{ii}$ is the shunt admittance, while E_i and J_i are the independent voltage and current sources due to the external excitation [10]. The controlled voltage and current sources represent the mutual coupling between different line segments. For the test case under examination,

Manuscript received November 19, 2016; revised January 18, 2017; accepted January 23, 2017. Date of publication January 31, 2017; date of current version May 26, 2017. Corresponding author: T. Campi (e-mail: tommaso.campi8888@gmail.com).

Color versions of one or more of the figures in this paper are available online at http://ieeexplore.ieee.org.

Digital Object Identifier 10.1109/TMAG.2017.2661859

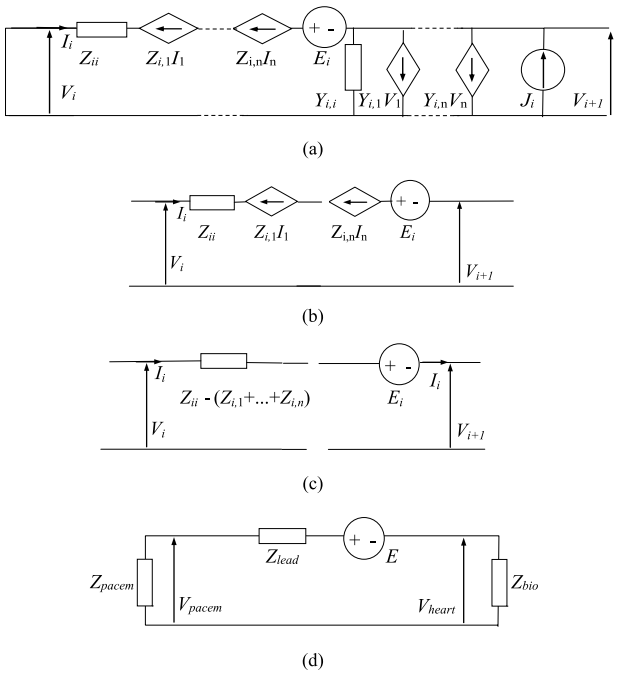

Fig. 2. Field excited circuit. (a) ith lumped circuit element. (b) ith lumped circuit element at LF when neglecting the transversal parameters. (c) ith lumped circuit element without controlled sources. (d) Equivalent circuit of the field excited pacing lead.

the equivalent circuit can be simplified by neglecting the shunt parameters, i.e., adopting the low-frequency (LF) approximation, as shown in Fig. 2(b).

This approximation is valid because the operational frequency ($f = 20$ kHz) is quite low, the lead is covered by dielectric insulation ($G_i \approx 0$), and the voltage is very small ($\omega C_i V_i \approx 0$, $J_i \approx 0$), as shown in Section IV. By the LF approximation, the current is the same in all lead sections ($I_1 = \ldots = I_i = \ldots = I_n = I$), and the series cascade of the circuit sections in Fig. 2(c) can be modeled by the simple circuit shown in Fig. 2(d). In such network, V_{pacem} represents the voltage at the input port of the pacemaker, V_{heart} the voltage in the heart, Z_{bio} the impedance of the current return path, Z_{pacem} the impedance at the input port of the pacemaker, and $Z_{lead} = R_{lead} + j\omega L_{lead}$ the impedance of the lead, where

$$R_{lead} = \sum_{i=1}^{n} R_i \tag{1a}$$

$$L_{lead} = \sum_{i=1}^{n} L_{ii} + \sum_{\substack{i,\, j = 1 \\ i \neq j}}^{n} s_{ij} M_{ij}\,. \tag{1b}$$

In (1b), L_{ii} is the partial self-inductance of the ith lead segment, M_{ij} is the partial mutual-inductance between the ith and jth lead segments, and s_{ij} represents the sign ($\pm$) of the particular partial inductance and depends on the direction of current flow in the ith and jth conductor segments [11], [12].

The circuit excitation in Fig. 2(d) is given by an electromagnetic force modeled as a voltage source E and given by

$$E = -j\omega\phi \tag{2}$$

where ϕ is the magnetic flux produced by the two coils of the WPT system and linked with the loop area. This flux

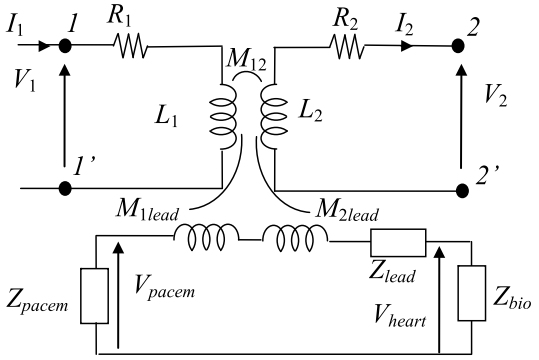

Fig. 3. Equivalent circuit of two WPT coils and an implanted pacemaker.

can be calculated as the surface integral of the magnetic field produced by the WPT current coils, when the overall configuration is analyzed by an EMF solver [1]–[3].

A different solution can be obtained by circuit simulation, when the voltage source E is given by

$$E = -j\omega M_{1,lead} I_1 - j\omega M_{2,lead} I_2 \tag{3}$$

where I_1 and I_2 are the currents flowing, respectively, in the primary and in the secondary coils of the WPT system, and $M_{1,lead}$ and $M_{2,lead}$ are the mutual inductances between the primary coil and the lead, and between the secondary coil and the lead, respectively. The equivalent circuit is shown in Fig. 3, where L_1 and L_2 represent the self-inductances of the WPT coils, M_{12} the coil mutual inductance, and R_1 and R_2 the coil resistances [1]–[3]. For simplicity, the source, loads, and compensation blocks of the WPT system are not reported in this figure.

B. Circuit Parameters Calculation

The lead internal wire has a helicoidal shape to increase its flexibility and mechanical robustness. Nevertheless, this shape has an impact on the electrical parameters as resistances and inductances. The self-inductance L_{ii} of any ith TL section into which the lead is discretized is given by $L_{ii} = L^i_{ii} + L^e_{ii}$, where L^i_{ii} is the internal inductance and L^e_{ii} the external inductance. The internal inductance L^i_{ii} and resistance R_i are experimentally obtained since the electro-geometrical configuration of the pacing lead is too complex to be calculated. The external self-inductances L^e_{ii} of the ith section are instead calculated using the expression of partial inductances for a cylindrical wire in free space. This expression can be assumed valid also inside the human body since all the biological tissues are characterized by a magnetic permeability $\mu = \mu_0$, and, at the frequency of interest, the power losses are negligible. Also the mutual inductance M_{ij} between the ith and the jth TL sections is calculated by the partial inductance theory. The formulas of the partial self- and mutual-inductances can be found in [11]–[14].

The mutual inductance between the planar spiral coils of the WPT system and the lead is obtained imposing a current $I_{lead} = 0$ on the lead and $I_{coil} \neq 0$ on the coils. The mutual inductance between the lead and the coil is given by

$$M_{coil,lead} = imag(V_{lead} / (j\omega I_{coil})) \tag{4}$$

where V_{lead} is the induced electromagnetic force on the lead.

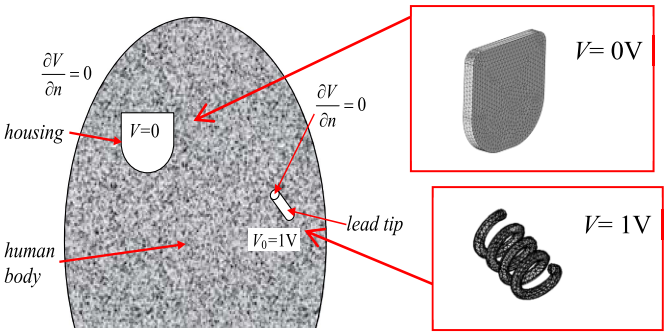

Fig. 4. Sketch of the field configuration used to calculate Z_{bio} and adopted meshes for the pacemaker and lead tip.

The circuit parameters of the WPT system in Fig. 3 can be numerically extracted or measured [1], [2]. The numerical extraction can also be successfully used for the calculation of the lead parameters instead of the use of partial inductances solving the magneto-quasi-static equations [2].

The calculation of the impedance Z_{bio} is strongly dependent on several aspects: the form and position of the two electrodes (pacemaker housing and lead tip in the heart) and the current path inside the inhomogeneous human body of complex shape. Since the analytical calculation is not possible, the impedance is numerically calculated solving the electro-quasi-static field equations in frequency domain by the finite element method using the commercial software COMSOL. The external surfaces of the helix shaped lead tip are made by perfectly electrical conductor, except for the bottom surface that is connected to the lead and is assumed to be electrically insulated in this instance. A voltage $V_0 = 1$ V is imposed on this electrode, while zero voltage is imposed on the external surfaces of the pacemaker case, as schematically shown in Fig. 4. For the 3-D simulations, a tetrahedral mesh with maximum element size comparable to a fraction of the skin depth has been adopted (see zoomed-in view of Fig. 4).

The current flowing into the two electrode surfaces (lead tip and housing) is calculated by postprocessing the field solution

$$I_{\text{tip}} = \int_{S_{\text{tip}}} \mathbf{J} \cdot d\mathbf{S} \tag{5a}$$

$$I_{\text{hous}} = \int_{S_{\text{hous}}} \mathbf{J} \cdot d\mathbf{S} \tag{5b}$$

where $\mathbf{J}$ is the current density vector, and S_{tip} and S_{hous} are the external conductive surfaces of the electrodes. It is easy to verify that $I_{\text{tip}} = -I_{\text{hous}} = I$, assuming a negligible numerical error. Thus, the return path impedance in biological tissues is calculated by

$$Z_{bio} = V_0/I \tag{6}$$

IV. Applications

The excitation to the pacing lead is given by the magnetic field produced by the current coils of the WPT charging system operating at the frequency $f_0 = 20$ kHz [1], [2]. To validate the excitation of the lead in the proposed method, the simplified setup shown in Fig. 5 has been realized. It is composed by a lead and a source coil in air. The magnetic

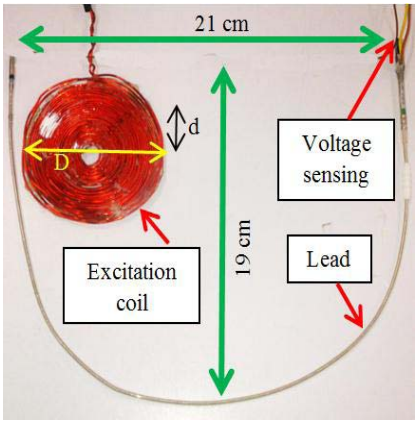

Fig. 5. Simplified setup in air for the validation of the numerical results.

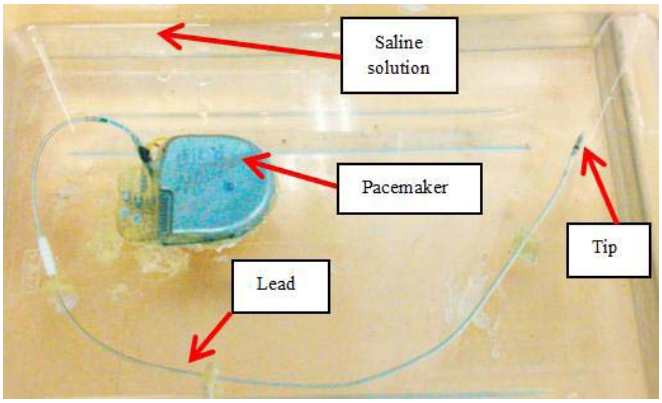

Fig. 6. Measurement setup configuration. The lead connected with the pacemaker housing has been immersed in a saline solution.

field excitation is generated by a sinusoidal current (1 A at 20 kHz) flowing into a planar spiral coil with outer diameter $D = 70$ mm, wire diameter $W = 1$ mm, and number of turns $N_t = 29$. The distance between the coil and the plane where the lead lies was set to $d = 1$ cm. For Faraday's Law, the time-harmonic magnetic flux in the loop formed by the curved unipolar pacing lead of 46-cm length gives rise to the induced voltage E coinciding with the open-ended voltage V_{pacem} when $Z_{pacem} = \infty$. This voltage was measured at the input port of the pacemaker and calculated. The measured and computed values were quite similar: $V_{pacem\_meas} = 55.0$ mV and $V_{pacem\_cal} = 52.1$ mV.

Then, a suitable setup for *in vitro* measurement was prepared as shown in Fig. 6. This setup consisted of a pacemaker housing with unipolar lead immersed in a saline solution characterized by a concentration of NaCl = 0.9% to simulate human tissues. The first test was performed to evaluate the correctness of the LF simplifying assumption (i.e., negligible transversal parameters in the circuit of Fig. 2(a). Thus, a 20 kHz current of 100 mA has been injected in a terminal of the lead while the current at the other lead terminal has been measured for different lead geometrical configurations. In all considered tests, the magnitude and phase of the measured currents at both terminals have revealed to be quite similar as shown in Fig. 7 confirming the correctness of the adopted LF approximation.

Finally, the induced voltage V_{pacem} due to the magnetic field produced by an external source coil was evaluated assuming a source coil having the same characteristics of the previous

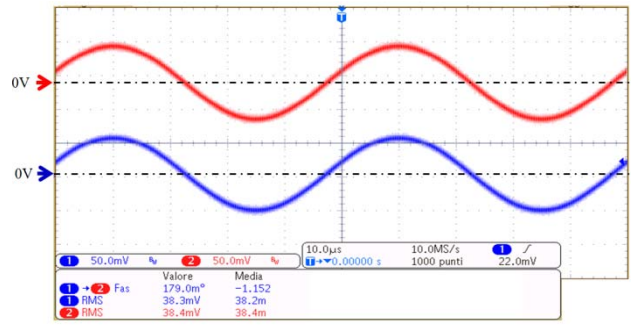

Fig. 7. Input (red) and output (blue) current waveforms on the lead immersed in a saline solution.

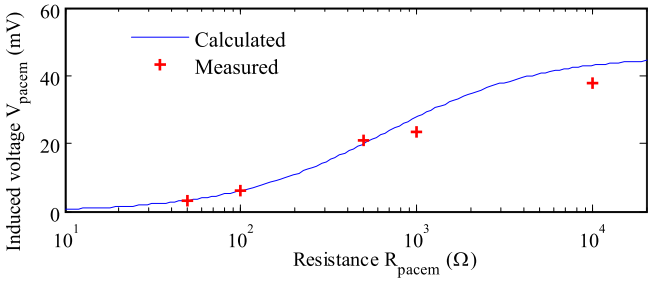

Fig. 8. Calculated and measured induced voltage V_{pacem} versus pacemaker input resistance R_{pacem}.

TABLE I
WPT PARAMETERS AND INDUCED VOLTAGE ON THE LEAD TERMINALS

	Calculated	Measured
Lead inductance L_{lead} (µH)	0.54	-
Mutual inductance $M_{coil,lead}$ (µH)	0.365	0.34
Lead resistance R_{lead} (Ω)	-	45
Resistance R_{bio} (Ω)	600	625
Coil inductance L_{coil} (µH)	27	30
Coil resistance R_{coil} (mΩ)	120	118
Induced voltage E (mV)	47.8	42.2

application. The voltage V_{pacem} was measured and calculated by the analysis of the equivalent circuit in Fig. 2(d). To this aim, first the impedances $Z_{lead} = R_{lead} + j\omega L_{lead}$, Z_{pacem}, and Z_{bio} were calculated. The lead inductance L_{lead} was computed using the partial inductances method [11]–[14], discretizing the lead into $n = 80$ line segments. The resistance R_{lead} was obtained by measurements at the frequency $f_0 = 20$ kHz. The computed and measured parameters of the circuit and the open loop ($I_{ind} = 0$) induced voltage E are shown in Table I.

At the considered frequency f_0, the impedance Z_{bio} is mainly resistive ($Z_{bio} \approx R_{bio}$) and its value is in the range 400–600 Ω, depending mainly on the tip configuration. Assuming a variable internal resistive impedance ($Z_{pacem} \approx R_{pacem}$) at the input port of the pacemaker (to consider various pacemaker type and settings), the voltage in the pacing lead has been calculated for several values of $R_{pacem} = 50$ Ω, 100 Ω, 500 Ω, 1 kΩ, and 10 kΩ.

Then V_{pacem} was measured using a high input impedance oscilloscope in the setup shown in Fig. 6. The obtained results for various values of R_{pacem} have been reported in Fig. 8. As can be observed, the numerical results are in satisfactory agreement with the measurements confirming the validity of the proposed approach to predict EMI in a very complex configuration.

V. CONCLUSION

The induced effects produced by the application of a WPT charging system to a pacemaker with a unipolar pacing lead has been evaluated for the first time. The proposed co-simulation approach allows a fast calculation of the induced voltage on the lead terminals produced by the WPT coil currents. The numerical results have been compared with measurements highlighting a satisfactory agreement. In the future, the obtained induced effects for real pacemaker configurations will be compared with standards limits. Furthermore, the proposed method will be applied to evaluate the EMI in bipolar leads.

REFERENCES

[1] T. Campi, S. Cruciani, V. De Santis, and M. Feliziani, "EMF safety and thermal aspects in a pacemaker equipped with a wireless power transfer system working at low frequency," *IEEE Trans. Microw. Theory Techn.*, vol. 64, no. 2, pp. 375–382, Feb. 2016.

[2] T. Campi, S. Cruciani, F. Palandrani, V. De Santis, A. Hirata, and M. Feliziani, "Wireless power transfer charging system for AIMDs and pacemakers," *IEEE Trans. Microw. Theory Techn.*, vol. 64, no. 2, pp. 633–642, Feb. 2016.

[3] S. Cruciani, T. Campi, F. Maradei, and M. Feliziani, "Numerical simulation of wireless power transfer system to recharge the battery of an implanted cardiac pacemaker," in *Proc. Int. Symp. Electromagn. Compat. (EMC EUROPE)*, Gothenburg, Sweden, vol. 4, pp. 44–47, Sep. 2014.

[4] T. Campi, S. Cruciani, V. De Santis, and M. Feliziani, "Immunity of a pacemaker with a wireless power transfer coil," in *Proc. Int. Symp. Electromagn. Compat. (EMC EUROPE)*, Wroclaw, Poland, pp. 290–293, Sep. 2016.

[5] T. Seckler *et al.*, "Effect of lead position and orientation on electromagnetic interference in patients with bipolar cardiovascular implantable electronic devices," *Europace*, vol. 19, no. 2, pp. 319–328, Feb. 2007.

[6] T. W. Dawson, K. Caputa, M. A. Stuchly, R. B. Shepard, R. Kavet, and A. Sastre, "Pacemaker interference by magnetic fields at power line frequencies," *IEEE Trans. Biomed. Eng.*, vol. 49, no. 3, pp. 254–262, Mar. 2002.

[7] *Active Implantable Medical Device. Part 1: General Requirements for Safety; Marking and Information to be Provided by the Manufactures*, document CEN EN 45502-1, 1997.

[8] *Active implantable Medical Device. Part 22: Particular Requirements for Active Implantable Medical Devices Intend to Treat Tachyarrhythmia (Includes Implantable Defibrillators)*, document CEN EN 45502-2-2, 2008.

[9] *Active Implantable Medical Devices—Electromagnetic Compatibility—EMC Test Protocols for Implantable Cardiac Pacemakers, Implantable Cardioverter Defibrillators and Cardiac Resynchronization Devices*, document ISO 14117, 2012.

[10] C. Taylor and C. Harrison, Jr., "The response of a terminated two-wire transmission line excited by a nonuniform electromagnetic field," *IEEE Trans. Antennas Propag.*, vol. 13, no. 6, pp. 987–989, Nov. 1965.

[11] S. Caniggia and F. Maradei, *Signal Integrity and Radiated Emission*. Hoboken, NJ, USA: Wiley, 2008.

[12] A. E. Ruehli, "Inductance calculations in a complex integrated circuit environment," *IBM J. Res. Develop.*, vol. 16, no. 5, pp. 470–481, Sep. 1972.

[13] C. R. Paul, "The concept of partial inductance," in *Inductance: Loop Partial*. Piscataway, NJ, USA: IEEE Press, pp. 195–245, 2010.

[14] L. Sandrolini, U. Reggiani, and G. Puccetti, "Analytical calculation of the inductance of planar zig-zag spiral inductors," *Prog. Electromagn. Res.*, vol. 142, pp. 207–220, Sep. 2013.